Chinese Chemical Letters 34 (2023) 108147

Contents lists available at ScienceDirect

Chinese Chemical Letters

journal homepage: www.elsevier.com/locate/cclet

Construction of sub-micron eccentric Ag@PANI particles by interface and redox potential engineering

Mingming Sun, Wei Guo*, Meiyu Meng, Qiuyu Zhang*

Key Laboratory of Special Functional and Smart Polymer Materials of Ministry of Industry and Information Technology, MOE Key Laboratory of Material Physics and Chemistry Under Extraordinary Conditions, School of Chemistry and Chemical Engineering, Northwestern Polytechnical University, Xi'an 710072, China

ARTICLE INFO

Article history:
Received 8 December 2022
Revised 27 December 2022
Accepted 11 January 2023
Available online 13 January 2023

Keywords:
Ag@PANI
Eccentric particles
Redox potential
Reaction interface
Microwave absorption

ABSTRACT

Benefitting from the tunable heterogeneous interface and electronic interaction, metal-polymer-based hybrid composites have attracted wide attention. It is highly desired to develop advanced synthesis methodology and understand the structure-performance relationship. Herein, with the aniline oligomer as the key enabler, we resolve the inferior dynamics issue in the Ag^+-aniline reaction system, and successfully fabricate a sub-micron anisotropic eccentric Ag@polyaniline (PANI) particle (an average size up to 340 nm) at room temperature. We demonstrate the synergy mechanism of polyvinyl pyrrolidone and *in-situ* generated PANI for modifying the dynamic reaction interface. We further clarify the H^+ concentration and the surfactant types serve as main descriptors to tune the reaction dynamics. Besides, by applying other aniline oligomers, a series of similar eccentric structures can also be obtained, indicative of the good applicability of our strategy. Such a sub-micron eccentric structure furnishes the Ag@PANI composites with sound performance for microwave absorption, as demonstrated by a minimum reflection loss (RL) value of −35 dB with an effective absorption bandwidth of 3.7 GHz. This study provides an inspiring scope/concept of eccentric microstructure engineering for better meeting the demands in the high-tech military, energy, environment fields, and beyond.

With the merits of unique heterointerface and organic/inorganic synergistic effects, metal@polymer core-shell materials generally demonstrate promising properties, such as high physicochemical stability [1,2], improved optical properties [3,4], enhanced catalytic activity [5], and fascinating interfacial properties [6]. Among them, Ag@polyaniline (PANI), integrated with the excellent conductivity and optical properties of Ag as well as low density, high mechanical flexibility and electrochemical properties of PANI, has been scrutinized as a promising hybrid material and investigated in many research fields [7–9]. Besides the "win-win cooperation", it has been evidenced that the modulation of organic/inorganic hybrid materials by rational design of their morphology and interface effects will further optimize the properties [10,11].

Anisotropic particles hold fascinating features such as asymmetric shapes and outstanding physicochemical properties [12], thus attracting considerable attention to date [13–15]. It is predicted that the precise configuration of Ag@PANI with an anisotropic microstructure will result in appealing features for wide applications [16,17]. However, the development of the well-defined anisotropic Ag@PANI structure is far behind schedule and challenging. Generally, the inferior processability of the organic component (PANI) renders it hard to finely couple with the metal materials to form the required microstructure [18–20]. On top of that, the low redox potential of Ag^+/Ag (0.80 V) to aniline (1.02 V) is the main bottleneck in the organic/inorganic hybrid system [21], which makes it thermodynamically unfavorable for the *in-situ* polymerization and the formation of Ag@PANI composites. To facilitate their development, rationally balancing the redox potential of aniline precursor to guarantee the facile and controllable synthesis at room temperature is highly pursued.

Generally speaking, aniline oligomers are formed at the early stage of the oxidation of aniline, with a shorter molecular chain and lower molecular weight [22]. Aniline oligomers, such as aniline trimer and tetramer, can serve as building blocks for the synthesis of PANI and other functional molecular structure [22,23]. Considering the lower redox potentials of aniline oligomers in comparison to that of aniline [24], it is expected that they may serve as the

* Corresponding authors.
E-mail addresses: weiguo-nwpu@nwpu.edu.cn (W. Guo), qyzhang@nwpu.edu.cn (Q. Zhang).

https://doi.org/10.1016/j.cclet.2023.108147
1001-8417/

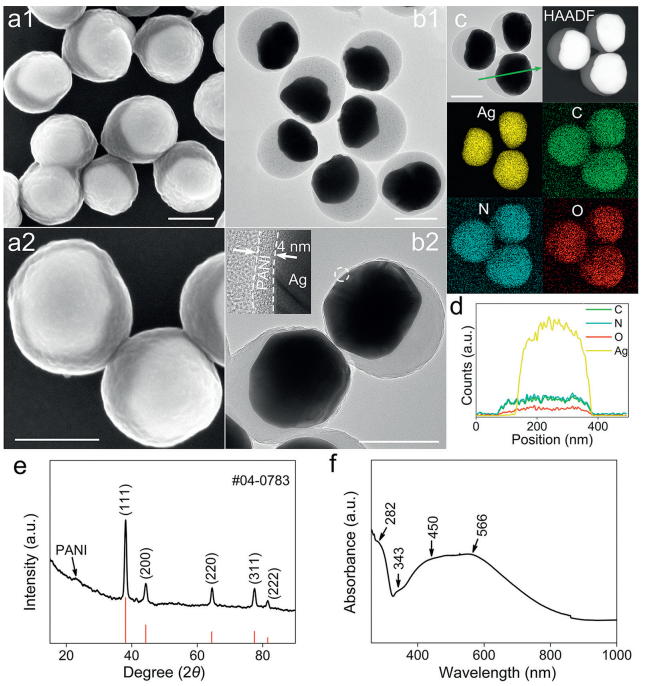

Fig. 1. (a1, a2) SEM images, (b1, b2) TEM images and (c) TEM and HAADF images of AP-Ag@PANI and the corresponding EDS elemental mapping, (d) line scanning (marked in c), (e) XRD pattern and (f) UV–vis-NIR spectrum of AP-Ag@PANI. Scale bar: 200 nm.

proper reductant of Ag^+, favorable for the polymerization and *in-situ* coupling with the as-formed Ag^0.

In this contribution, inspired by the aforementioned information, aniline oligomers are adopted as the reductants in the organic/inorganic hybrid system, which lead to the successful formation of sub-micron eccentric Ag@PANI particles. We clarify that the polyvinyl pyrrolidone (PVP) is responsible for the modified reaction interface of appropriate microdroplets owing to its amphipathic groups. We also reveal that the *in-situ* generated PANI as the hydrophobic layer on the Ag particle will be engulfed in the oil context gradually, leading to the homogeneous growth of eccentric Ag@PANI. More interestingly, the similar eccentric structure synthesized by different precursors of aniline oligomers demonstrates the good applicability of our strategy. It is proposed that a growth process is controlled by the joint effect of the reaction interface and diffusion kinetics, where the main descriptors are revealed. The geometric and interface synergy renders the eccentric Ag@PANI particles with superior performance when used as a microwave absorber, where a minimum reflection loss (RL) value of −35 dB at 10.5 GHz and an effective absorption bandwidth of 3.7 GHz (RL value < −10 dB) are realized. This work provides a successful formation craft of sub-micron metal-polymer eccentric particles, which helps advance the design and modulation of functional materials for diverse application scenarios.

As illustrated in Fig. S1 (Supporting information), the aniline oligomers were formed with ammonium persulfate (APS) or Ag^+ as the oxidizer, namely AP-precursor and AG-precursor, respectively. Both of them perform high-activity of reducing Ag^+ ions towards the generation of Ag@PANI structures at room temperature.

In a typical reaction with AP-precursor, we obtained eccentric AP-Ag@PANI particles with an average size of about 340 nm (Figs. 1a and b, Fig. S2 in Supporting information). The AP-Ag@PANI particle possesses a highly eccentric Ag core in an irregular shape, encapsulated by the spherical PANI shell with a small nanotextured surface. The anisotropic coating thicknesses of the PANI shell for the thin and thick sides are 4 nm and above 100 nm, respectively. HRTEM image (Fig. S3 in Supporting information) demonstrates a lattice spacing is 0.23 nm, which can be indexed to the (111) plane of metallic Ag. Besides, the selected area electron diffraction (SAED) pattern demonstrates the polycrystalline structure of the eccentric particle (inset in Fig. S3). The unique morphology was also demonstrated by the high-angle annular dark-field scanning TEM (HAADF-STEM) image (Fig. 1c). Besides, the corresponding energy dispersive spectroscopy (EDS) mapping and the line scanning demonstrate an even distribution of C, N and O elements from the PANI shell and Ag element from the core (Figs. 1c and d).

To further investigate the crystal structure of AP-Ag@PANI, X-ray diffraction (XRD) characterization was conducted. As shown in Fig. 1e, five distinct diffraction peaks can be detected, ascribed to the (111), (200), (220), (311) and (222) planes of Ag (JCPDS No. 04–0783), respectively. Besides, a weak peak in the range of 20°-30° is observed, originating from the PANI shell [25]. The optical property was characterized by UV–vis-NIR spectroscopy. As shown in Fig. 1f, three characteristic bands at 282, 343 and 566 nm stem from PANI, assigned to a π-π^* transition of benzenoid (B) rings, π-π^* transition and molecular exciton for polyaniline, respectively [26,27]. The localized surface plasmon resonance (LSPR) peak at 450–480 nm is associated with the inner Ag core. These results manifest that Ag particles are successfully immobilized within the polyaniline matrix. To evidence the applicability of this strategy, we performed a contrast experiment where the AG-precursor was used as a reductant. As a result, eccentric AG-Ag@PANI particles with an average size of about 210 nm were obtained (more details in Figs. S2 and S4 in Supporting information). These results validate that we can utilize aniline oligomers oxidized by diverse oxidants to fabricate special eccentric structures.

The composite structures were further investigated by FTIR measurement as shown in Fig. 2a. The peaks at 3354 and 3359 cm^{-1} are assigned to the N–H stretching vibrations of PANI [28]. The peaks at 2927 and 2849 cm^{-1} are ascribed to the C–H stretching vibrations of PANI [29]. The peaks at 1467 and 1597 cm^{-1} can be attributed to the C=C stretching vibrations of B and quinonoid (Q) rings, respectively [29]. The peak at 1384 cm^{-1} is assigned to C–N stretching vibration in the bipolaronic and polaronic units [29]. And the strong band at 1638 cm^{-1} corresponds to the stretching of C=O group, attributed to the hydrolysis of PANI [30]. The peaks at 1293 and 1306 cm^{-1} are attributed to the N–H bending mode [31]. The Raman spectra of the AP-Ag@PANI and AG-Ag@PANI nanocomposites (Fig. 2b) display a series of characteristic peaks of PANI in emeraldine salt form. Specifically, the peaks at 870 and 1160 cm^{-1} can be attributed to the C–H bending vibration of the Q and B rings, respectively [29]. The peaks at 1252 and 1352 cm^{-1} are ascribed to the C–N stretching vibration of the polaronic and bipolaronic moieties, respectively [29]. The peak of about 1384 cm^{-1} is assigned to C∼$N^{\bullet+}$ stretching vibration of the polaronic moieties [32]. The peak of about 1430 cm^{-1} is attributed to C=N stretching vibration of the Q rings [32]. The two peaks of about 1592 and 1624 cm^{-1} originate from the C=C and C–C stretching vibrations of the Q and B rings, respectively [29]. The shoulder band of about 1660 cm^{-1} is assigned to the C=O stretching vibration from the hydrolysis of PANI. The band of 246 cm^{-1} can be attributed to the Ag-N band among PANI and Ag particles (Fig. S5 in Supporting information) [33].

XPS characterization was performed to gain some insights into the electronic structure of the as-synthesized eccentric structures. For both AP-Ag@PANI and AG-Ag@PANI, the characteristic peaks of C, N and O elements were detected, manifesting the introduction of PANI (Fig. 2c). As shown in Fig. 2d, the spectra of the Ag 3d consist of two spin-orbit components Ag $3d_{5/2}$ and Ag $3d_{3/2}$ at 367.6 and 373.6 eV with an energy separation of 6.0 eV, confirm-

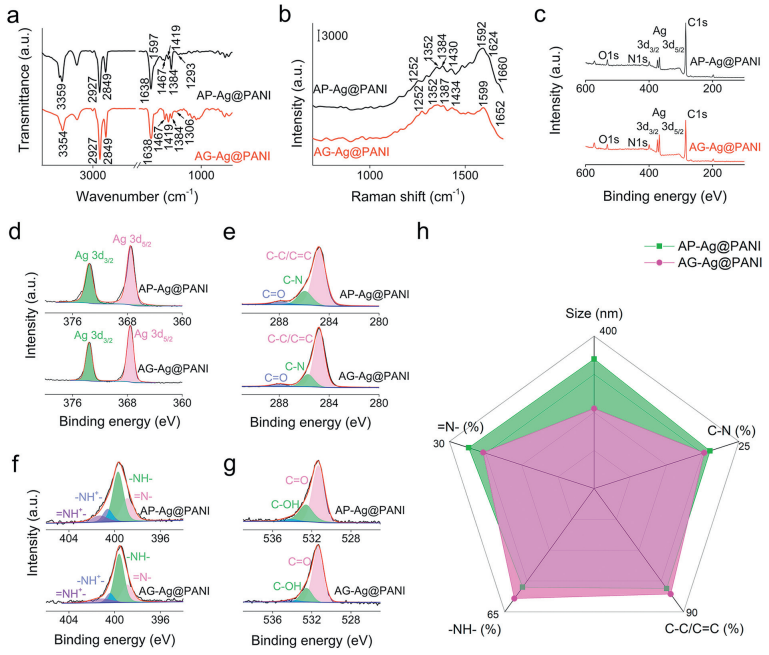

Fig. 2. (a) FTIR spectra, (b) Raman spectra, (c) XPS survey spectra, (d) high-resolution Ag 3d XPS spectra, (e) C 1s XPS spectra, (f) N 1s XPS spectra, (g) O 1s XPS spectra and (h) the comparison of different groups percentage and size of AP-Ag@PANI and AG-Ag@PANI, respectively.

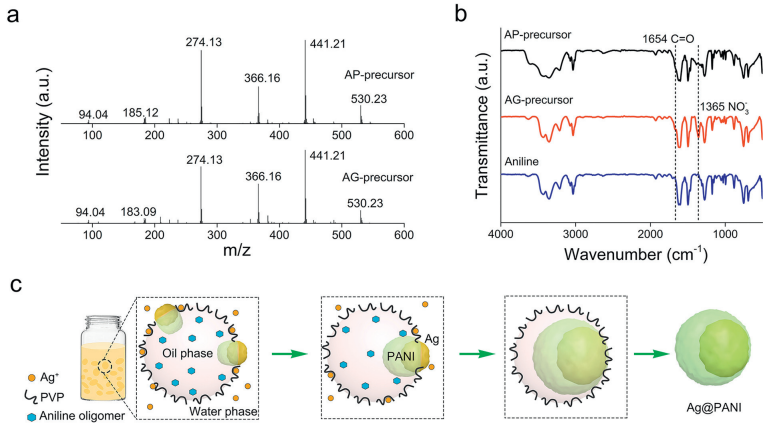

Fig. 3. (a) TOF-MS of AP-precursor and AG-precursor, (b) FTIR spectra of AP-precursor, AG-precursor and pure aniline, and (c) schematic diagram of the proposed formation process of eccentric Ag@PANI structure in an oil/water biphasic system.

ing the average valence state of 0 [34]. It evidences the successful formation of Ag particles. The high-resolution C 1s XPS spectra of AP-Ag@PANI and AG-Ag@PANI can be divided into three distinct peaks at 284.8, 285.7 and 288.0 eV, originating from C–C/C=C, C–N and C=O bonds, respectively (Fig. 2e). The N 1s spectra are deconvoluted into four component peaks at 398.9, 399.6, 400.4 and 401.1 eV, assigned to =N-, -NH-, $-NH^+$- and $=N^+$-, respectively (Fig. 2f) [29]. The presence of protonated nitrogen suggests that the PANI was obtained in the emeraldine salt form. The O 1s spectra can be deconvoluted into three subpeaks at 531.3, 532.6 and 534.1 eV, which are assigned as C=O, C–OH and chemisorbed oxygen and/or water bonding states, respectively (Fig. 2g). As depicted in Fig. 2h, the aforementioned results demonstrate that the relative group contents display negligible difference for AP-Ag@PANI and AG-Ag@PANI, further manifesting the great promise of this redox potential-matching strategy.

The mass spectrometry of the aniline precursors was studied to understand their composition. As shown in Fig. 3a and Fig. S6 (Supporting information), aniline ($m/z = 94.04$), aniline dimer ($m/z = 185.12$), trimer ($m/z = 274.13$) and tetramer ($m/z = 366.16$) were detected [35]. Moreover, the fragments at $m/z = 441.21$ and 530.23 arise from the pentamer and hexamer, with a loss of $NH_2^{\bullet}$ [35,36]. The FTIR spectra of both AP-precursor and AG-precursor exhibit an extra C=O band ($1654\,cm^{-1}$) compared with the pure aniline, indicative of the existence of PVP residues in the aniline precursors (Fig. 3b).

As mentioned above, the special biphasic system composed of the oil phase (aniline oligomers in toluene) and water phase (Ag^+ and H^+ in water), is the key to fabricated eccentric Ag@PANI structure (Fig. 3c). After blending the oil and water phases, there are numerous microdroplets with the assistance of PVP from the aniline oligomers, which serve as the reaction centers. Notably, Ag^+ ions are easily absorbed on PVP [37], further initiating the polymerization of oligomers. Due to the high activity of aniline oligomers, Ag^+ ions will be fast reduced and grow into primary Ag particles. Subsequently, the *in-situ* formed PANI will coat the surface of Ag particles and be embedded in the oil phase owing to their hydrophobicity [38]. Then, Ag particles further grow and

are coated with swollen PANI shells. Finally, the eccentric Ag@PANI composites formed after the Ag particle was engulfed in the PANI matrix. The formation process of the eccentric Ag@PANI structure is also proven by the defective products as shown in Fig. S7 (Supporting information).

It was demonstrated that the PVP played a key role in the system. Without PVP, the as-formed Ag@PANI particles exhibit irregular shapes and small sizes (Figs. S8a and b in Supporting information), originating from the unstable oil/water interface of micelles in the absence of PVP. The effect on the reaction interface was further studied by adding appropriate sodium dodecyl benzene sulfonate (SDBS) instead of PVP as the surfactant. The uneven Ag@PANI particle structure with thin shells is formed (Fig. S8c in Supporting information), which may come from small micelles assisted by SDBS. That is to say, the PVP, which is conducive to fabricating appropriate microdroplets and stabilizing oil-water interfaces [39], serves as a significant role in manufacturing the eccentric Ag@PANI structure.

To gain more insights on the formation of eccentric Ag@PANI structure, the reaction was further conducted under different H^+ concentrations with consideration of tuning the nucleation of PANI [40]. Under a high concentration (80 mmol/L), more than one core inside the PANI shell was observed the as-formed AP-Ag@PANI particles (Fig. S8d in Supporting information). It indicates that the potential interaction of adjacent AP-Ag@PANI particles appears, due to the accelerated reaction as the increased protonation of aniline oligomers under high H^+ concentration. As the H^+ concentration further increases to 120 mmol/L (Fig. S8e in Supporting information), the obtained AP-Ag@PANI particles exhibit ordinary core-shell structure with agglomeration, originating from the fast reaction between Ag^+ and aniline oligomers. Besides, there was no obvious product under a low H^+ concentration of 30 mmol/L because of the inadequate protonation of aniline oligomers. Therefore, the types of surfactants and the H^+ concentration are two main descriptors (Fig. S8f in Supporting information), contributing to modulating the interfaces of microdroplets and the reaction kinetics, respectively.

AP-Ag@PANI was adopted as the microwave absorbent to evaluate the microwave absorption (MA) property of this kind of special eccentric structure by the RL value. The pure PANI only exhibits the maximal absorption of −12 dB with an effective absorption bandwidth of 3.4 GHz (Figs. 4a and b, Fig. S9 in Supporting information). By contrast, the eccentric AP-Ag@PANI particles exhibit an absorption of −22 dB with an effective MA bandwidth of 3.5 GHz under a sample thickness of only 1.5 mm (Figs. 4c and d). More importantly, the maximal absorption reaches −35 dB at the frequency of 10.4 GHz under a sample thickness of only 2.1 mm, and the effective absorption bandwidth of 3.7 GHz is achieved (from 9.3 GHz to 13.0 GHz). Encouragingly, this absorption efficiency is higher than many previously reported Ag-polymer-based materials in literature (Fig. S10 in Supporting information), indicative of the good potential of these eccentric AP-Ag@PANI nanostructures as a high-performance microwave absorber.

To clarify the origin of the enhanced microwave absorption, the permittivity of these eccentric AP-Ag@PANI nanostructures was evaluated. As shown in Figs. S11a and b (Supporting information), the high value of ε' suggests a high electric storage capability [41]. Besides, the high value of ε'' also manifests that the special eccentric structure of AP-Ag@PANI can enhance the dissipation loss of electromagnetic energy [41]. The dielectric loss value ($\tan\delta_\varepsilon = \varepsilon''/\varepsilon'$) of AP-Ag@PANI is displayed in Fig. S11c (Supporting information), indicative of a high dielectric loss of electromagnetic waves. As shown in Fig. S11d (Supporting information), there are several semicircles from the Cole-Cole plot of ε' and ε'' of AP-Ag@PANI, which are related to the Debye relaxation process due to the interface polarization between Ag nanoparticle and PANI [42].

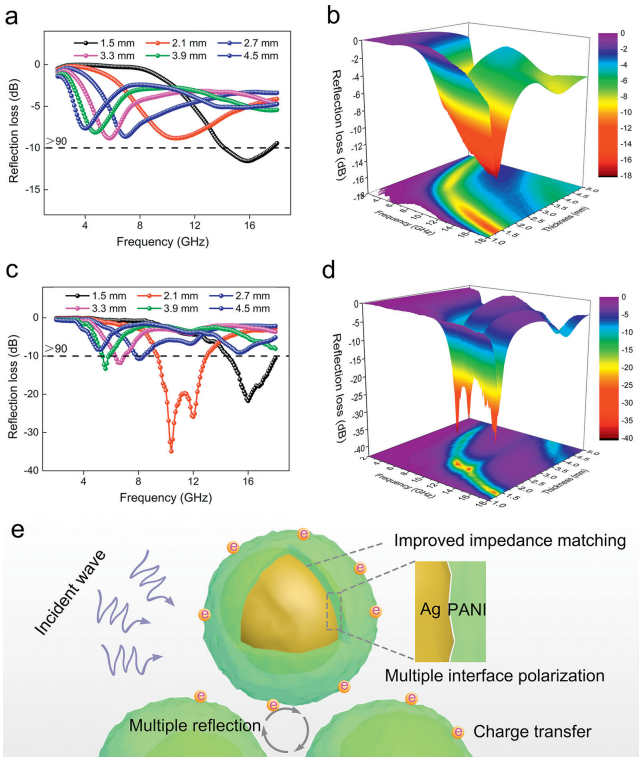

Fig. 4. (a, c) Reflection loss curves and (b, d) three-dimensional reflection loss representations of the pure PANI and AP-Ag@PANI. (e) Schematic illustration of the absorption mechanism of eccentric Ag@PANI composites.

Moreover, AP-Ag@PANI exhibits high impedance matching, owing to the excellent microwave absorption performance (Fig. S11e in Supporting information) [43]. Therefore, both the high dielectric loss and sound impedance match contribute to enhanced absorption performance.

The underlying mechanisms for the excellent absorption performance of the eccentric AP-Ag@PANI structure are summarized (Fig. 4e). First, the eccentric AP-Ag@PANI structure shows an enhanced impedance matching characteristic compared with pure Ag particles. This enables more microwaves to get in and facilitates the contact interaction between the microwaves and the AP-Ag@PANI [41]. Also, thanks to the abundant Ag/PANI hybrid interfaces, interfacial polarization and the corresponding relaxation further enlarge the dielectric loss and microwave absorption performance. Besides, the special eccentric AP-Ag@PANI can introduce multiple reflections, which would ensure the efficient attenuation of the incident microwave. Moreover, the electromagnetic waves are attenuated through the charge transfer course in the Ag/PANI interfaces. Generally speaking, the enhanced microwave absorption performance is primarily accredited to the novel eccentric Ag@PANI structure and the related interfacial effect between Ag and PANI components.

In summary, through the precise modulation of redox potential and the dynamic reaction interface, we have successfully synthesized the sub-micron eccentric Ag@PANI particles at room temperature. Our strategy shows sound applicability, evidenced by the successful formation of similar eccentric structures with different aniline oligomers as the precursors. We have further revealed that the surfactant types and H^+ concentration serve as the main descriptors of the formation of eccentric Ag@PANI composites by modulating the reaction interface and kinetic process, respectively. The growth process of the eccentric Ag@PANI, guided by the PVP-modulated dynamic reaction interface, has been refined as three steps: (1) the initial nucleation & growth of small Ag particles, (2)

the *in-situ* coating of PANI, accompanied by further growth of Ag to form Ag@PANI, and (3) the generation of large Ag@PANI with Ag particle fully engulfed. The special eccentric composite with multiple interfaces as well as the synergetic effect of Ag and PANI feature excellent MA performance, such as a minimum RL value of −35 dB and an effective absorption bandwidth of 3.7 GHz. With the advanced modulation/manipulation strategy in terms of microstructure and surface chemistry of the metal@polymer system, this work is believed to facilitate the development of promising and novel functional materials to meet different requirements.

Declaration of competing interest

The authors declare no conflict of interest.

Acknowledgments

The authors are grateful for the support and funding from the National Natural Science Foundation of China (Nos. 51673156, 52202301), the Natural Science Basic Research Plan in Shaanxi Province of China (No. 2022JQ-143), China Postdoctoral Science Foundation (No. 2022TQ0256) and the Fundamental Research Funds for the Central Universities (No. D5000210607).

Supplementary materials

Supplementary material associated with this article can be found, in the online version, at doi:10.1016/j.cclet.2023.108147.

References

[1] S. Wu, M. Zhu, Q. Lian, et al., Nanoscale 10 (2018) 18565–18575.
[2] L. Tzounis, M. Doña, J. Lopez-Romero, A. Fery, R. Contreras-Caceres, ACS Appl. Mater. Interfaces 11 (2019) 29360–29372.
[3] J. Zhou, J.W. J.eon, J. Ponder, et al., J. Mater. Chem. C 5 (2017) 12571–12584.
[4] J. Wang, C. Zhu, J. Han, et al., ACS Appl. Mater. Interfaces 10 (2018) 12323–12330.
[5] C. Kirubaharan, G. Kumar, C. Sha, et al., Electrochim. Acta 328 (2019) 135136.
[6] Z. Wu, H. Cheng, C. Jin, et al., Adv. Mater. 34 (2022) 2107538.
[7] Z. Chen, F. Zhang, Y. Lu, et al., Chin. Chem. Lett. 33 (2022) 3144–3150.
[8] H. Xu, J. Li, P. Li, et al., ACS Appl. Mater. Interfaces 13 (2021) 49194–49205.
[9] M. Deshmukh, B. Kang, T. Ha, J. Mater. Chem. C 8 (2020) 5112–5123.
[10] P. Xiong, Y. Wu, Y. Liu, et al., Energy Environ. Sci. 13 (2020) 4834–4853.
[11] J. Zhou, B. Duan, Z. Fang, et al., Adv. Mater. 26 (2014) 701–705.
[12] C. Chen, L. Xie, Y. Wang, Nano Res. 12 (2019) 1267–1278.
[13] J. Feng, F. Yang, X. Wang, et al., Adv. Mater. 31 (2019) 1900789.
[14] B. Liu, S. Thanneeru, A. Lopes, et al., Small 13 (2017) 1700091.
[15] D. Liu, N. Yang, Q. Zeng, et al., Chin. Chem. Lett. 32 (2021) 3288–3297.
[16] R. Li, H. Wang, Y. Song, et al., J. Am. Chem. Soc. 141 (2019) 19542–19545.
[17] H. Lv, D. Xu, L. Sun, et al., Nano Lett. 19 (2019) 3379–3385.
[18] C. Baker, X. Huang, W. Nelson, R. Kaner, Chem. Soc. Rev. 46 (2017) 1510–1525.
[19] G. Wang, P. Hao, Y. Chang, et al., Nanoscale 14 (2022) 2256–2265.
[20] A. Abouelsayed, B. Anis, W. Eisa, J. Phys. Chem. C 124 (2020) 18243–18256.
[21] S. Pillalamarri, F. Blum, A. Tokuhiro, M. Bertino, Chem. Mater. 17 (2005) 5941–5944.
[22] T. Ghosh, U. Basak, P. Bairi, et al., ACS Appl. Nano Mater. 3 (2020) 1693–1705.
[23] Y. Ye, D. Yang, D. Zhang, et al., Chem. Eng. J. 383 (2020) 123160.
[24] W. Li, H. Wang, J. Am. Chem. Soc. 126 (2004) 2278–2279.
[25] L. Zhao, K. Wang, W. Wei, L. Wang, W. Han, InfoMat 1 (2019) 407–416.
[26] J. Kinyanjui, D. Hatchett, J. Smith, M. Josowicz, Chem. Mater. 16 (2004) 3390–3398.
[27] P. Paulraj, N. Janaki, S. Sandhya, K. Pandian, Colloids Surf. A 377 (2011) 28–34.
[28] K. Mallick, M. Witcomb, A. Dinsmore, M. Scurrell, Macromol. Rapid Commun. 26 (2005) 232–235.
[29] N. Dianat, M. Rahmanifar, A. Noori, et al., Nano Lett. 21 (2021) 9485–9493.
[30] Q. Zhang, A. Zhou, J. Wang, J. Wu, H. Bai, Energy Environ. Sci. 10 (2017) 2372–2382.
[31] J. Lee, Y. Jang, W. Xu, et al., J. Mater. Chem. A 5 (2017) 13692–13699.
[32] M. Trchová, Z. Morávková, J. Dybal, J. Stejskal, ACS Appl. Mater. Interfaces 6 (2014) 942–950.
[33] G. Xiao, S. Man, Chem. Phys. Lett. 447 (2007) 305–309.
[34] S. Li, L. Xie, G. Luo, et al., Chin. Chem. Lett. 33 (2022) 551–556.
[35] H. Deng, G.J. V.an Berkel, Anal. Chem. 71 (1999) 4284–4293.
[36] S.W. W.alker, A. Mark, B. Verbuyst, et al., J. Phys. Chem. A 122 (2018) 3858–3865.
[37] D. Chen, M. Liu, Q. Chen, et al., Appl. Catal. B 144 (2014) 394–407.
[38] J. Ge, Y. Hu, T. Zhang, Y. Yin, J. Am. Chem. Soc. 129 (2007) 8974–8975.
[39] B. Guo, J. Zhao, C. Wu, et al., Colloids Surf. B 177 (2019) 346–355.
[40] J. Stejskal, I. Sapurina, M. Trchová, E. Konyushenko, Macromolecules 41 (2008) 3530–3536.
[41] A. Xie, K. Zhang, M. Sun, Y. Xia, F. Wu, Mater. Des. 154 (2018) 192–202.
[42] J. Li, D. Zhou, P. Wang, W. Liu, J. Su, J. Mater. Chem. A 8 (2020) 20337–20345.
[43] X. Li, L. Yu, W. Zhao, et al., Chem. Eng. J. 379 (2020) 122393.